ENGINEERING COMPUTATIONS, VOL. 10, 323–336 (1993)

AN EFFECTIVE TECHNIQUE FOR MODELLING 2D METAL FORMING PROCESSES USING AN EULERIAN FORMULATION

EDUARDO N. DVORKIN AND EVA G. PETÖCZ

Center for Industrial Research, FUDETEC, Av. Córdoba 320, 1054 Buenos Aires, Argentina

ABSTRACT

In order to develop an engineering tool for modelling 2D metal forming processes we implemented in the flow formulation the pseudo-concentrations technique and a quadrilateral element based on mixed interpolation of tensorial components (QMITC). By doing this we obtained a reliable and efficient Eulerian formulation for modelling steady and transient metal forming problems. Some cases were analysed in order to test the performance of the formulation.

KEY WORDS QMITC Eulerian Metal forming products

INTRODUCTION

For modelling industrial metal forming processes the use of rigid-viscoplastic[1] material models in the flow formulation[2–4] is usually a very effective and reliable engineering option. Although residual stresses and elastic spring-back effects are not predicted using the flow formulation, the results provided by this formulation have proved to be very accurate for forming load and plastic strain predictions as well as for the prediction of the velocity distribution throughout the domain of the problem.

In this paper we present several finite element techniques that we use in our implementation of the flow formulation in order to improve the quality and efficiency of the computational predictions.

In the following sections we will discuss:

- a finite element formulation apt for modelling incompressible rigid-viscoplastic problems;
- a free surface algorithm for stationary problems that does not move nodes and therefore avoids the need for remeshing;
- an algorithm for modelling transient processes, for materials with or without strain-hardening, using an Eulerian formulation in a fixed or arbitrarily moving mesh. This Eulerian formulation avoids element distortions and therefore the need for remeshing usually encountered in the Eulerian–Lagrangian techniques;
- an algorithm for solving frictional contact problems.

In the last section we present some numerical experimentation to illustrate the behaviour of the presented computational techniques.

0264-4401/93/040323-14$2.00

Received May 1992
Revised October 1992

THE QMITC ELEMENT

Using the technique of *m*ixed *i*nterpolation of *t*ensorial *c*omponents (MITC), the quadrilateral QMITC element was developed for elasto-plastic problems (Lagrangian description of motion[5,6]). With the objective of using the QMITC element with the flow formulation (Eulerian description of motion) to model metal forming processes, the QMITC element was implemented for the analysis of 2D incompressible Stokes flow in Reference 7.

In this formulation we use:

- the penalty method to impose the incompressibility constraint;
- the velocity interpolation corresponding to a 5-node isoparametric element[8,9]. The velocity degrees of freedom corresponding to the central node are condensed at the element level;
- the following interpolations for the strain-rate components:

$$\hat{\dot{\varepsilon}}_{ii} = \hat{\dot{\varepsilon}}_{ii}|_O^{DI} + \frac{\sqrt{3}}{2}[\hat{\dot{\varepsilon}}_{ii}|_D^{DI} - \hat{\dot{\varepsilon}}|_B^{DI}]\frac{|J_0|}{|J|}r + \frac{\sqrt{3}}{2}[\hat{\dot{\varepsilon}}|_A^{DI} - \hat{\dot{\varepsilon}}|_C^{DI}]\frac{|J_0|}{|J|}s \tag{1a}$$

where $i = r, s$ for plane strain-rate problems and $i = r, s, t$ for axisymmetric problems.

$$\hat{\dot{\varepsilon}}_{rs} = \hat{\dot{\varepsilon}}_{rs}|_O^{DI} \tag{1b}$$

In the above, $\hat{\dot{\varepsilon}}_{ij}|_{A,B,C,D,O}^{DI}$ are the covariant strain-rate components at sampling points A, B, C, D and O, evaluated from the velocity interpolation and referred to the contravariant base vectors at the element centre. The sampling points natural coordinates are $A(0, 1/\sqrt{3})$, $B(-1/\sqrt{3}, 0)$, $C(0, -1/\sqrt{3})$, $D(1/\sqrt{3}, 0)$, $O(0, 0)$. $|J_0|$ is the determinant of the element Jacobian at point O. $|J|$ is the determinant of the element Jacobian at the point of natural coordinates (r, s).

The QMITC element in incompressible Stokesian flows presents the following features[7]:

- the element does not contain any spurious zero energy mode[8,9];
- the element satisfies Irons' patch test[9];
- the element does not lock either in plane or axisymmetric strain-rate problems[10];
- the predictive capabilities of the element are very insensitive to distortions;
- the oscillations in the pressure solution (checkerboard) tend to zero as the mesh is refined[9];
- the element presents predictive capabilities comparable to higher order u/p and penalty elements.

An accurate modelling of metal forming processes requires the use of the rigid-viscoplastic Perzyna-type constitutive equation (1) with an associate flow rule (maximum viscoplastic dissipation) and the von Mises yield function (incompressible flow). The QMITC incompressible Stokes flow formulation, fulfilling the above requirements, is apt for modelling metal forming processes.

A FREE SURFACE ALGORITHM FOR STATIONARY PROBLEMS

We use a free surface algorithm based on the pseudo-concentrations technique developed by Thompson[11,12]. This algorithm describes free surfaces inside a fixed mesh, avoiding mesh distortions usually associated to standard free surface algorithms[4] and therefore avoiding the need for remeshing procedures.

The pseudo-concentrations technique assigns a pseudo-concentration to each node (c_i for $i = 1, \ldots, N$) (e.g. $c_i > 0$ indicates that material is present at node i while $c_i < 0$ indicates the absence of material therefore if $c_i = 0$ node i is on the free surface[11–13]). The

Table 1 Solution algorithm for stationary problems

I. Initial guess for pseudo-concentrations: $c^{(0)}$
II. Equilibrium equations:

$$\mathbf{K}(c^{(0)})\mathring{\mathbf{U}}^{(0)} = \mathbf{R}$$

III. Reference unbalanced power:

$$\mathring{E}_{\mathrm{REF}} = [\mathring{\mathbf{U}}^{(0)}]^{\mathrm{T}}\mathbf{R}$$

IV. $i = 1$
V. Advection equation for pseudo-concentrations:

$$\mathring{\mathbf{u}}^{(i-1)} \cdot \nabla c^{(i)} = 0 \Rightarrow \overset{\circ}{c}{}^{(i)}$$

VI. Equilibrium equations:

$$\mathbf{K}(c^{(i)}, \mathring{\mathbf{U}}^{(i-1)})\Delta\mathring{\mathbf{U}}^{(i)} = \mathbf{R} - \mathbf{F}^{(i-1)}(c^{(i)}, \mathring{\mathbf{U}}^{(i-1)})$$

$$\mathring{\mathbf{U}}^{(i)} = \mathring{\mathbf{U}}^{(i-1)} + \Delta\mathring{\mathbf{U}}^{(i)}$$

VII. Unbalanced power:

$$\mathring{E}_i = [\Delta\mathring{\mathbf{U}}^{(i)}]^{\mathrm{T}} \cdot [\mathbf{R} - \mathbf{F}^{(i-1)}]$$

VIII. IF ($\mathring{E}_i < \mathrm{ETOL} \cdot \mathring{E}_{\mathrm{REF}}$) THEN
GO TO IX
ELSE
$i = i + 1$
GO TO V
IX. $\mathring{\mathbf{U}} = \mathring{\mathbf{U}}^{(i)}$
$\mathring{\mathbf{u}} \cdot \nabla c = 0 \Rightarrow c$
X. Calculate $\dot{\varepsilon}$ and σ
XI. END

pseudo-concentrations are interpolated inside the QMITC element using the interpolation functions of a 4-node isoparametric element (h_i for $i = 1, \ldots, 4$)[8,9]:

$$c = \sum_{i=1}^{4} h_i c_i \tag{2}$$

In general the free surfaces ($c = 0$) will be interior to the elements.

When solving the equilibrium equations, for element points where $c > 0$ we use the actual material properties while for element points where $c < 0$ we use an artificial (low) viscosity (e.g. $\nu_{\mathrm{actual}} = \nu/1000$).

Given a velocity distribution ($\mathring{\mathbf{u}}$) in the mesh that satisfies the incompressibility condition ($\nabla \cdot \mathring{\mathbf{u}} = 0$), the pseudo-concentrations must satisfy the advection equation:

$$\mathring{\mathbf{u}} \cdot \nabla c = 0 \tag{3}$$

For the solution of (3) we make use of the upwinding procedure described in Reference 14.

In *Table 1* we present our iterative algorithm for the solution of stationary problems.

TRANSIENT PROBLEMS

For solving transient problems using the flow formulation, Eulerian–Lagrangian methods are usually implemented[4]. In these methods the mesh is updated in each incremental step and remeshing procedures are necessary when the element distortions reach an unacceptable level.

Instead of using an Eulerian–Lagrangian formulation we implemented an Eulerian formulation. We model transient problems using Thompson's pseudo-concentrations technique[11,13]. For this purpose we either use a fixed mesh or a mesh moving with an arbitrary velocity field ($\mathring{\mathbf{u}}_m$) that satisfies the geometrical boundary conditions.

The transport equation for the pseudo-concentrations is, for an incompressible flow:

$$\frac{\partial c}{\partial t} + (\mathring{\mathbf{u}} - \mathring{\mathbf{u}}_m)\cdot\nabla c = 0 \tag{4}$$

For the integration of (4) we use either the upwinding procedure[15,16] (conditionally stable) or the Crank–Nicholson algorithm[17] (unconditionally stable).

Many researchers found out that after integrating (4) for the incremental time step from time (load level) t to time (load level) $t + \Delta t$ the use of a smoothing algorithm is necessary. In our

Table 2 Solution algorithm for transient problems

I. Data: ${}^t c, {}^t\bar{\varepsilon}, {}^t\mathring{\mathbf{U}}$

$${}^{t+\Delta t}c^{(0)} = {}^t c$$

$${}^{t+\Delta t}\bar{\varepsilon}^{(0)} = {}^t\bar{\varepsilon}$$

II. Equilibrium equations:

$$\mathbf{K}({}^t c, {}^t\mathring{\mathbf{U}}, {}^t\bar{\varepsilon})[{}^{t+\Delta t}\mathring{\mathbf{U}}^{(0)} - {}^t\mathring{\mathbf{U}}] = {}^{t+\Delta t}\mathbf{R} - {}^t\mathbf{F}({}^t c, {}^t\mathring{\mathbf{U}}, {}^t\bar{\varepsilon})$$

III. Reference unbalanced power:

$${}^{t+\Delta t}\mathring{E}_{\mathrm{REF}} = [{}^{t+\Delta t}\mathring{\mathbf{U}}^{(0)} - {}^t\mathring{\mathbf{U}}]^{\mathrm{T}}\cdot[{}^{t+\Delta t}\mathbf{R} - {}^t\mathbf{F}]$$

IV. $i = 1$

V. Transport equation for pseudo-concentrations:

$$\frac{\partial^{t+\Delta t}c^{(i)}}{\partial t} + [{}^{t+\Delta t}\mathring{\mathbf{u}}^{(i-1)} - \mathring{\mathbf{u}}_M]\cdot\nabla^{t+\Delta t}c^{(i)} = 0 \Rightarrow {}^{t+\Delta t}c^{(i)}$$

VI. Transport equation for the equivalent plastic strain:

$$\frac{\partial^{t+\Delta t}\bar{\varepsilon}^{(i)}}{\partial t} + [{}^{t+\Delta t}\mathring{\mathbf{u}}^{(i-1)} - \mathring{\mathbf{u}}_M]\nabla^{t+\Delta t}\bar{\varepsilon}^{(i)} = \left\langle \frac{{}^{t+\Delta t}c^{(i)}}{\|{}^{t+\Delta t}c^{(i)}\|} \right\rangle {}^{t+\Delta t/2}\mathring{\bar{\varepsilon}}^{(i)} \Rightarrow {}^{t+\Delta t}\bar{\varepsilon}^{(i)}$$

VII. Equilibrium equations:

$$\mathbf{K}({}^{t+\Delta t}c^{(i)}, {}^{t+\Delta t}\mathring{\mathbf{U}}^{(i-1)}, {}^{t+\Delta t}\bar{\varepsilon}^{(i)})\Delta^{t+\Delta t}\mathring{\mathbf{U}}^{(i)} = {}^{t+\Delta t}\mathbf{R} - {}^{t+\Delta t}\mathbf{F}^{(i-1)}({}^{t+\Delta t}c^{(i)}, {}^{t+\Delta t}\mathring{\mathbf{U}}^{(i-1)}, {}^{t+\Delta t}\bar{\varepsilon}^{(i)})$$

$${}^{t+\Delta t}\mathring{\mathbf{U}}^{(i)} = {}^{t+\Delta t}\mathring{\mathbf{U}}^{(i-1)} + \Delta^{t+\Delta t}\mathring{\mathbf{U}}^{(i)}$$

VIII. Unbalanced power:

$${}^{t+\Delta t}\mathring{E}_i = [\Delta^{t+\Delta t}\mathring{\mathbf{U}}^{(i)}]^{\mathrm{T}}\cdot[{}^{t+\Delta t}\mathbf{R} - {}^{t+\Delta t}\mathbf{F}^{(i-1)}]$$

IX. IF $({}^{t+\Delta t}\mathring{E}_i < \mathrm{ETOL}\cdot{}^{t+\Delta t}\mathring{E}_{\mathrm{REF}})$ THEN
GO TO X
ELSE
$i = i + 1$
GO TO V

X. ${}^{t+\Delta t}\mathring{\mathbf{U}} = {}^{t+\Delta t}\mathring{\mathbf{U}}^{(i)}$

$$\frac{\partial^{t+\Delta t}c}{\partial t} + [{}^{t+\Delta t}\mathring{\mathbf{u}} - \mathring{\mathbf{u}}_M]\cdot\nabla^{t+\Delta t}c = 0 \Rightarrow {}^{t+\Delta t}c$$

$$\frac{\partial^{t+\Delta t}\bar{\varepsilon}}{\partial t} + [{}^{t+\Delta t}\mathring{\mathbf{u}} - \mathring{\mathbf{u}}_M]\cdot\nabla^{t+\Delta t}\bar{\varepsilon} = \left\langle \frac{{}^{t+\Delta t}c}{\|{}^{t+\Delta t}c\|} \right\rangle {}^{t+\Delta t/2}\mathring{\bar{\varepsilon}} \Rightarrow {}^{t+\Delta t}\bar{\varepsilon}$$

XI. Calculate ${}^{t+\Delta t}\sigma$

XIII. END

numerical experimentation we found that if the initial distribution of pseudo-concentrations ($t = 0$) is smooth enough, then no smoothing algorithm is necessary. This is a very important aspect for the computational efficiency of the method.

For tracking the equivalent viscoplastic strain $\bar{\varepsilon}$, and therefore the strain-hardening, at any point we solve the following equation:

$$\frac{D\bar{\varepsilon}}{Dt} = \frac{\partial \bar{\varepsilon}}{\partial t} + (\dot{\mathbf{u}} - \dot{\mathbf{u}}_m)\cdot\nabla\bar{\varepsilon} = \left\langle \frac{c}{\|c\|} \right\rangle \dot{\bar{\varepsilon}} \tag{5}$$

where $\dot{\bar{\varepsilon}}$ is the equivalent viscoplastic strain-rate and,

$$\langle x \rangle = \begin{cases} x & \text{for } x \geqslant 0 \\ 0 & \text{for } x < 0 \end{cases}$$

The solution procedure for (5) is analogous to that of (4) with the addition of a source term, treated consistently with the Petrov–Galerkin approach[18].

In *Table 2* we present our incremental iterative algorithm for the solution of transient problems.

THE FRICTIONAL CONTACT PROBLEM

Friction

Between pairs of frictional surfaces we consider the constant friction law[2–4,19]:

$$\tau_f = -m\frac{\sigma_y}{\sqrt{3}}\,\mathrm{sgn}(\dot{\mathbf{u}}_r\cdot\mathbf{t}) \tag{6}$$

where m is the friction coefficient ($0 \leqslant m \leqslant 1$), $\dot{\mathbf{u}}_r$ is the relative velocity between the two surfaces and $\mathbf{t}$ is the tangent unit vector to the surfaces.

In order to improve the numerical behaviour of the algorithm we use instead of (6) the following approximation[2]:

$$\tau_f = -m\frac{\sigma_y}{\sqrt{3}}\frac{2}{\pi}\tan^{-1}\left(\frac{\dot{\mathbf{u}}_r\cdot\mathbf{t}}{\text{scale}}\right) \tag{7}$$

where scale is a numerical factor that in our implementation is taken as:

$$\text{scale} \cong 10^{-2}\dot{U}$$

in the above $\dot{U}$ is a characteristic interface tangential velocity for the problem under consideration.

Contact

In order to prevent the effects of the incompressibility of the artificial material ($c < 0$) when it gets trapped, we consider contact boundary conditions for $\dot{\mathbf{u}}_n$ (normal relative velocity) of the form:

$$\dot{u}_n = \text{free} \quad \text{for } c < 0 \tag{8a}$$

$$\dot{u}_n = 0 \quad \text{for } c \geqslant 0 \tag{8b}$$

In the case of sticking condition at the wall, the two degrees of freedom are suppressed if $c \geqslant 0$.

In *Figure 1a* we show the results for a problem of mould filling obtained imposing as contact boundary conditions $\dot{\mathbf{u}}_n = 0$ during the complete solution procedure; it is evident the effect of

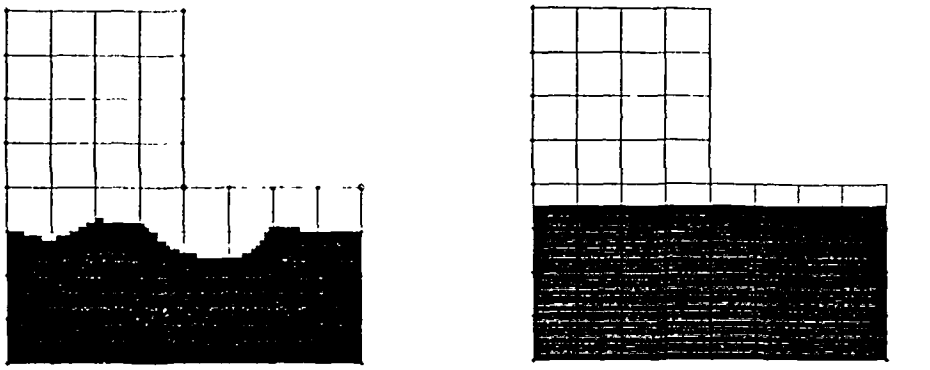

Figure 1 Artificial bubbles in a mould filling problem

the spurious 'artificial material bubbles' that get trapped. In *Figure 1b* we show the results obtained using the c-dependent boundary conditions (8): no 'artificial material bubbles' are present.

On the other hand, the c-dependent boundary conditions can cause a loss of the actual material because the velocity is only set to zero once the material has already reached the boundary. In the numerical example for mould filling we investigate the magnitude of this error, showing that it can be reduced to a very small value.

NUMERICAL EXPERIMENTATION

In this section we present several examples aimed at illustrating the behaviour of the presented finite element techniques.

Stationary problems

Swelling of Newtonian and polymeric flows. In *Figure 2* we present the results we obtained for the swelling of plane and axisymmetric flows, considering the following material law:

$$\mu = \mu_0 \dot{\bar{\varepsilon}}^{n-1}$$

In the above $n = 1.0$ corresponds to a Newtonian fluid. Our results are compared with those published in Reference 20.

Rolling of a perfectly-plastic sheet. For analysing this problem we make two simplifications: rigidly-perfectly plastic material; 2D plane strain-rate flow.

At the roll we employ the constant friction law (7) with $m = 1.0$ (maximum possible friction).

In *Figure 3a* we illustrate the dimensions ($h = 0.8$ and roll radius $= 5.5$) for our case and the velocity boundary conditions; in *Figure 3b* we illustrate the pseudo-concentration boundary conditions and in *Figure 3c* we show the QMITC mesh.

We have analysed the case for several values of the velocity at the entry and obtained the following results for each case (maintaining the roll angular velocity): the pseudo-concentrations distribution; the value of the inlet traction; the pressure distribution on the roll.

In *Figure 3d* we show the pseudo-concentrations distribution for one of the analysed cases.

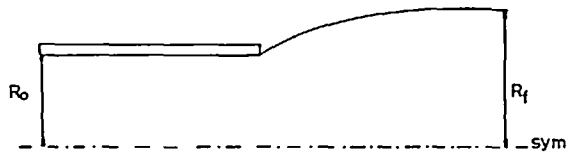

(a) the swelling problem

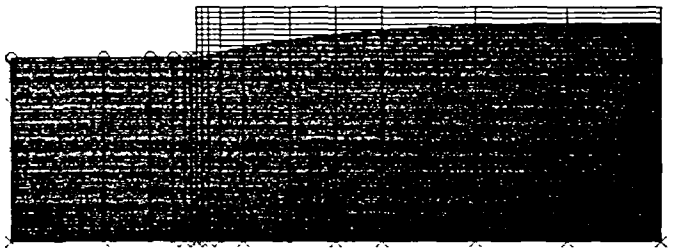

	Rf/Ro
This work	1.187
Ref. [20]	1.190±0.002

(b) results for a Newtonian fluid in plane flow

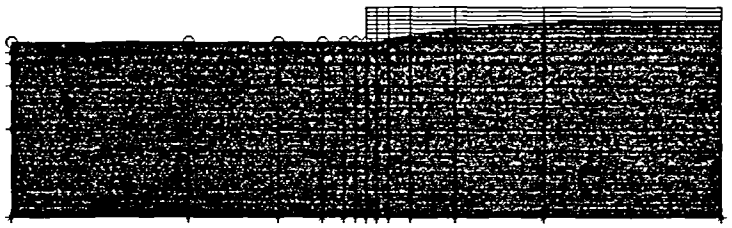

(c) results for a Newtonian fluid in axisymmetric flow

	Rf/Ro	
n	Ref.[20]	This work
1.0	1.127	1.133
0.7	1.072	1.074
0.5	1.040	1.040

(d) results for a polymeric fluid in axisymmetric flow

Figure 2 Swelling problems

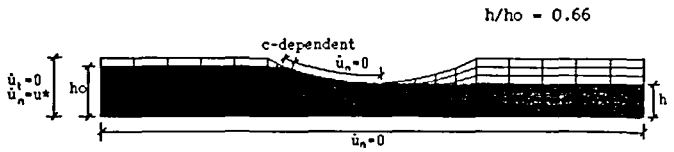

(a) dimensions and velocity boundary conditions

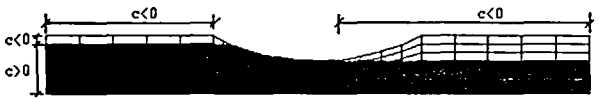

(b) pseudo-concentrations boundary conditions

(c) mesh used

(d) pseudo-concentrations distribution for $\sigma_{in}=-1.204\ \sigma_o$

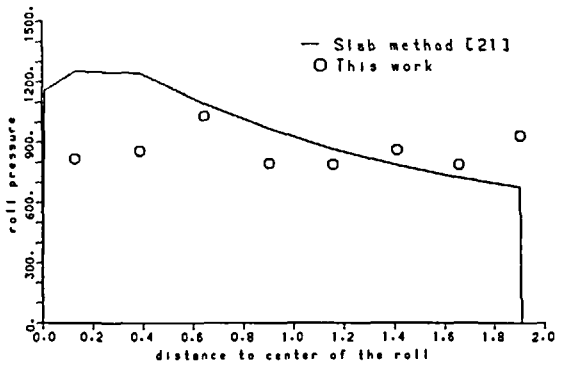

(e) pressure on the roll for $\sigma_{in}=0.504\ \sigma_o$

(f) pressure on the roll for $\sigma_{in}=0.060\ \sigma_o$

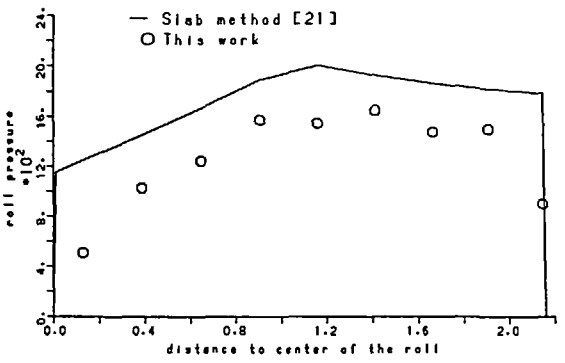

(g) pressure on the roll for $\sigma_{in}=-0.653\ \sigma_o$

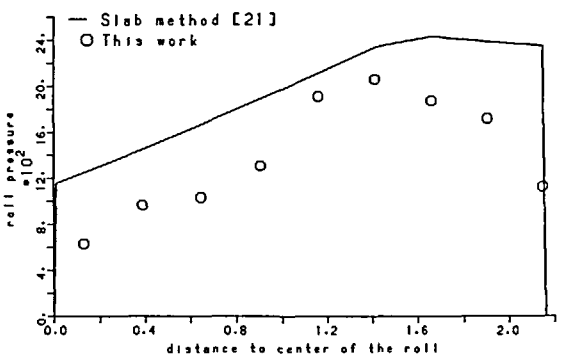

(h) pressure on the roll for $\sigma_{in}=-1.204\ \sigma_o$

Figure 3 Rolling of a perfectly plastic sheet

In *Figures 3e* to *3h* we present our solution for the pressure distribution on the rolls for several values of the inlet traction (σ_{in}/σ_0, where σ_0 is the yield stress) compared to the approximate solution obtained using the slab method[21].

Transient problems

Filling of a mould. In this problem we simulate the injection of a power law fluid into an axisymmetric mould[22]. For this fluid:

$$\mu = \mu_0 \bar{\dot{\varepsilon}}^{(n-1)/2}$$

and for the analysed case $n = 0.0$.

In *Figures 4a* to *4c* we show the fluid penetration into the mould at three different times, and in *Figure 4d* we show the error in the volume conservation at different time steps.

This is an interesting problem to test the accuracy we can expect using the c-dependent boundary conditions in (8). This accuracy is measured by the volume conservation.

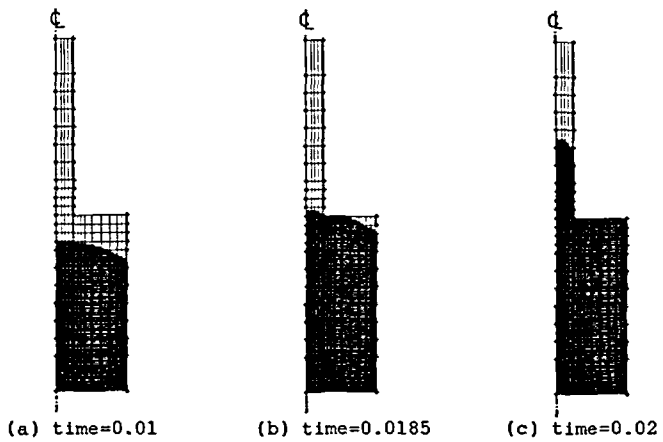

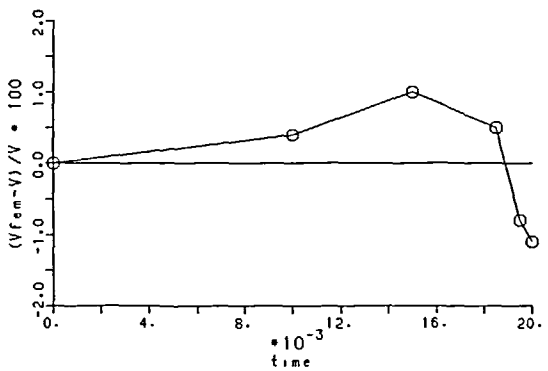

(d) error in volume conservation

Figure 4 Filling of an axisymmetric mould

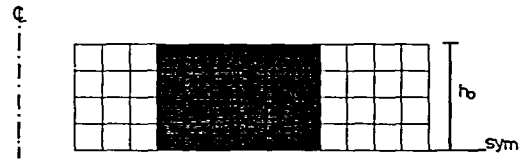

(a) mesh used

(b) resultant configuration for h/ho=0.54 and m=0.5

(c) resultant configuration for h/ho=0.54 and m=1.0

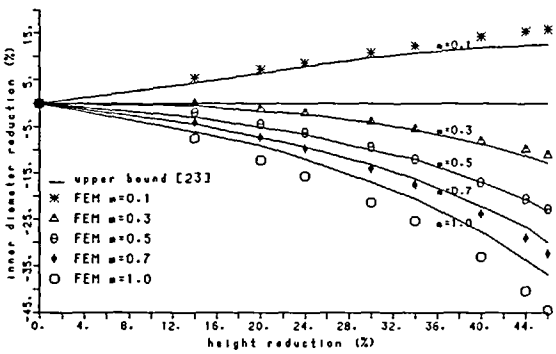

(d) calibration curves

Figure 5 Ring compression (perfectly plastic material)

Ring compression test (perfectly plastic material). In *Figure 5* we present our results for a ring compression test considering a rigid-perfectly plastic material and a 6:3:2 (outer diameter:inner diameter:height) ring geometry. Our results are compared with the upper-bound results published in Reference 23. It is important to point out that, for the FEM solution the inner radius was measured in the transverse symmetry plane.

Ring compression test (work hardening material). In *Figure 6* we present our results for a ring compression (6:3:2) considering a rigid-plastic material with the following hardening law:

$$\sigma_y = \sigma_0(1 + 0.81\bar{\varepsilon})$$

and a friction coefficient $m = 1.0$.

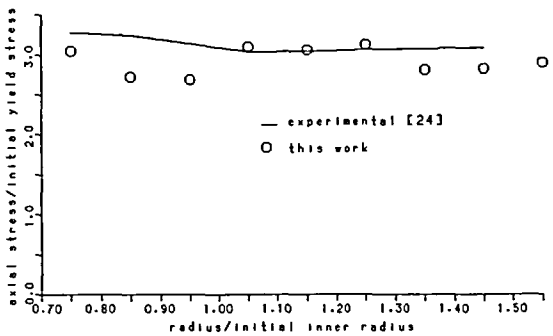

(a) compression stresses corresponding to a 45% reduction

Reduction in height (%)	Reduction in inner radius (%)	
	Experimental [24]	This work
40	46	42.8

(b) inner radius

Figure 6 Ring compression (work-hardening material)

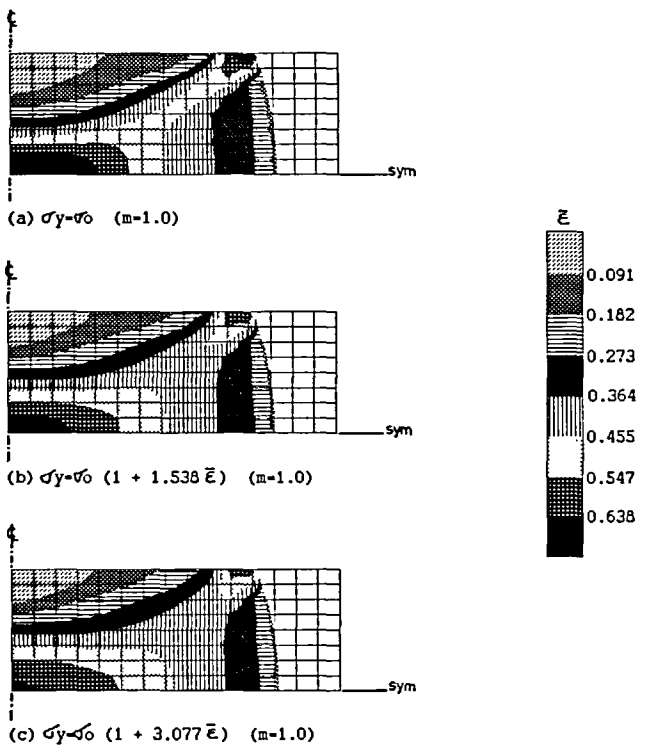

Figure 7 Compression of a cylinder. Equivalent plastic strain distribution ($\bar{\varepsilon}$) for a 30% reduction

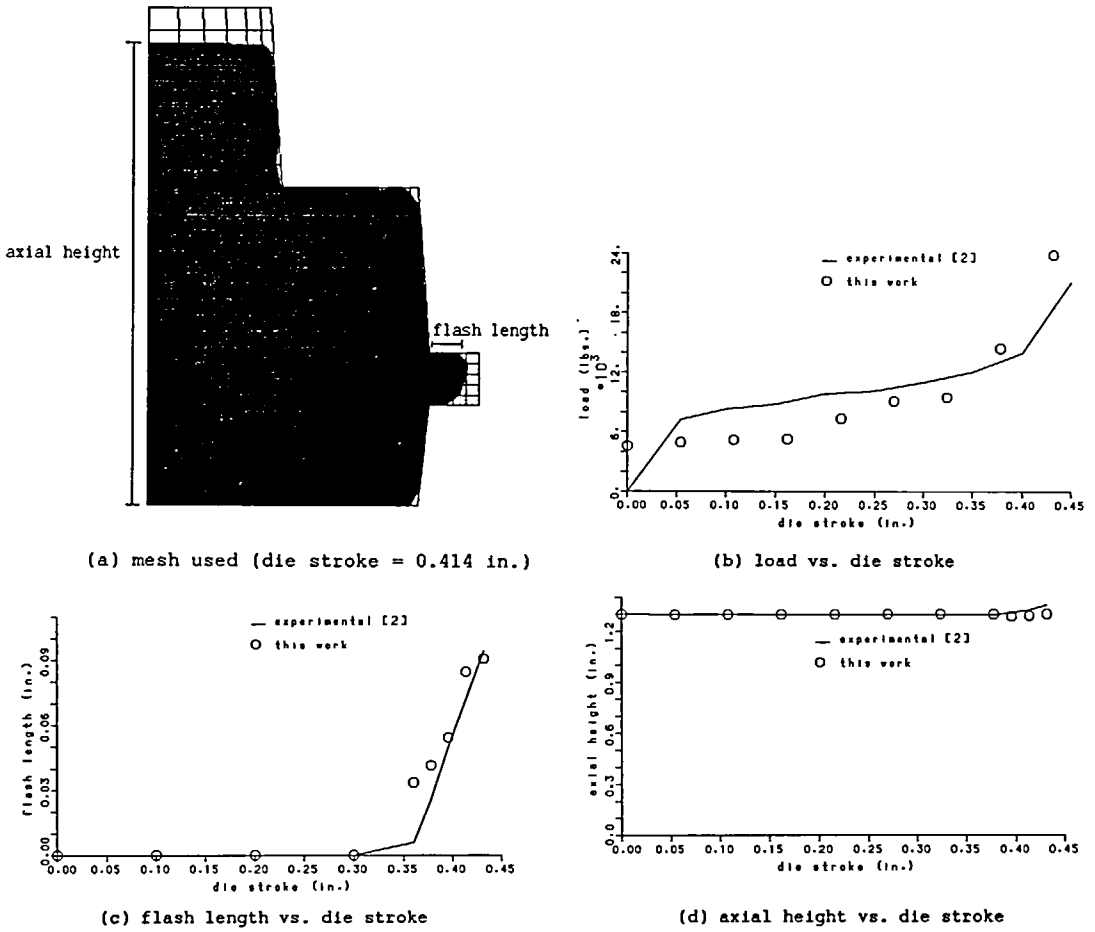

Figure 8 Closed die forging

Our results are compared with the experimental results published in Reference 24.

Compression of a cylinder (work hardening material). In *Figure 7* we show our results for the equivalent plastic strain distribution corresponding to three different hardening moduli.

It is evident that an increase in the work hardening modulus causes a decrease in the plastic strain localization.

Forging with closed dies. For this problem shown in *Figure 8* a rigid-perfectly plastic material was considered and a maximum friction condition ($m = 1.0$) at the walls was used.

Our results are compared with the experimental results published in Reference 2.

CONCLUSIONS

In order to develop a reliable and efficient engineering tool for modelling 2D metal forming processes we implemented in the flow formulation the quadrilateral QMITC element and the

pseudo-concentrations technique developed by Thompson obtaining an Eulerian formulation for modelling steady and transient problems.

In this paper we discuss:

(1) the QMITC element formulation which fulfils all the requirements for a reliable modelling of incompressible Stokes flows: no spurious zero energy modes, satisfaction of Irons' patch test, no locking behaviour, a high predictive capability and very insensitive to element distortions. Regarding this last point it is important to point out that: it was shown[25] that for elements with only eight exterior degrees of freedom, insensitivity to element distortions is competitive with satisfaction of Irons' patch test. In this regard we decided to strictly satisfy the patch test; by adding interior degrees of freedom[26] the element performance can be improved, but increasing the computational cost. In this regard we decided to add only two interior degrees of freedom[5].
(2) A free surface algorithm for stationary problems based on the pseudo-concentrations technique. This algorithm does not alter the elements geometry by moving nodes.
(3) An algorithm for transient problems also based on the pseudo-concentrations technique. This algorithm can consider materials with strain-hardening characteristics and uses an Eulerian formulation avoiding therefore mesh distortions.
(4) An algorithm for solving frictional contact problems.

The numerical results presented in the previous section show that the implemented technique for modelling metal forming processes using an Eulerian formulation[27] is very reliable and efficient.

ACKNOWLEDGEMENT

We gratefully acknowledge the support of SIDERCA (Campana, Argentina) for this research under the program 'Seamless steel tubes upsetting processes'.

REFERENCES

1 Perzyna, P. Fundamental problems in viscoplasticity, *Advances in Applied Mechanics*, Vol. 9, Academic Press, New York (1966)
2 Chen, C. C. and Kobayashi, S. Rigid-plastic finite element analysis of plastic deformation in metal-forming processes, *Tech. Rep. AFML-TR-79-4105*, Wright-Patterson Air Force Base (1979)
3 Zienkiewicz, O. C., Jain, P. C. and Oñate, E. Flow of solids during forming and extrusion: some aspects of numerical solutions, *Int. J. Solid Struct.* **14**, 15–28 (1977)
4 Zienkiewicz, O. C. Flow formulation for numerical solution of forming processes, in *Numerical Analysis of Forming Processes* (Eds J. F. T. Pittman *et al.*), John Wiley, Chichester (1984)
5 Dvorkin, E. N. and Vassolo, S. I. A quadrilateral 2D finite element based on mixed interpolation of tensorial components, *Eng. Comput.* **6**, 217–224 (1989)
6 Dvorkin, E. N. and Assanelli, A. P. Elasto-plastic analysis using a quadrilateral 2D element based on mixed interpolation of tensorial components, *Proc. Second International Conference on Computational Plasticity* (Eds. D. R. J. Owen *et al.*), Pineridge Press, Swansea, pp. 263–283 (1990)
7 Dvorkin, E. N. and Canga, M. E. Incompressible viscoplastic flow analysis using a quadrilateral 2D element based on mixed interpolation of tensorial components, *Commun. Num. Meth. Eng.* **9**, 157–164 (1993)
8 Bathe, K. J. *Finite Element Procedures in Engineering Analysis*, Prentice-Hall, Englewood Cliffs, NJ (1982)
9 Zienkiewicz, O. C. and Taylor, R. L. *The Finite Element Method*, 4th Edn, Vol. 1, McGraw-Hill, New York (1989)
10 Naagtegal, J. C., Parks, D. M. and Rice, J. R. On numerically accurate finite element solutions in the fully plastic range, *Comput. Meth. Appl. Mech. Eng.* **4**, 153–177 (1974)
11 Thompson, E. Use of the pseudo-concentrations to follow creeping viscous flows during transient analysis, *Int. J. Num. Meth. Fluids* **6**, 749–761 (1986)
12 Thompson, E. and Smelser, R. E. Transient analysis of forging operations by the pseudo-concentrations method, *Int. J. Num. Meth. Eng.* **23**, 177–189 (1988)

13 Antúnez, H. J., Idelsohn, S. E. and Dvorkin, E. N. Metal forming analysis by Fourier series expansion and further uses of pseudo-concentrations, *Comp. Struct.* **44**, 435–451 (1992)
14 Zienkiewicz, O. C., Heinrich, O. C., Huyakorn, J. C. and Mitchell, A. An upwind finite element scheme for two-dimensional convective transport equation, *Int. J. Num. Meth. Eng.* **11**, 131–143 (1977)
15 Yu, C. C. and Heinrich, J. C. Petrov–Galerkin methods for the time dependent convective transport equation, *Int. J. Num. Meth. Eng.* **23**, 883–901 (1986)
16 Yu, C. C. and Heinrich, J. C. Petrov–Galerkin method for multidimensional, time dependent, convective–diffusion equations, *Int. J. Num. Meth. Eng.* **24**, 2201–2215 (1987)
17 Crandall, S. H. *Engineering Analysis*, McGraw-Hill, New York (1956)
18 Brooks, A. N. and Hughes, T. J. R. Streamline upwind Petrov–Galerkin formulations for convection dominated flows with particular emphasis on the incompressible Navier–Stokes equations, *Comput. Meth. Appl. Mech. Eng.* **32**, 199–259 (1982)
19 Backofen, W. A. *Deformation Processing*, Addison-Wesley, Reading, MA (1972)
20 Tanner, R. I. Problems and progress in polymer extrusion studies, in *Numerical Analysis of Forming Processes* (Eds J. F. T. Pittman *et al.*), John Wiley, Chichester (1984)
21 Tselikov, A. *Stress and Strain in Metal Rolling*, Mir Publishers, Moscow (1967)
22 Matsuhiro, I., Shiojima, T., Shimazaki, Y. and Daiguji, H. Numerical analysis of polymer injection moulding process using finite element method with marker particles, *Int. J. Num. Meth. Eng.* **30**, 1569–1576 (1990)
23 Avitzur, B. *Metal Forming: The Application of Limit Analysis*, Marcel Dekker, New York (1980)
24 Mahrenholtz, O. Different finite element approaches to large plastic deformations, *Comput. Meth. Appl. Mech. Eng.* **33**, 453–468 (1982)
25 MacNeal, R. H. A theorem regarding the locking of tapered four-noded membrane elements, *Int. J. Num. Meth. Eng.* **24**, 1793–1799 (1987)
26 Pian, T. H. H. and Sumihara, K. Rational approach for assumed stress finite elements, *Int. J. Num. Meth. Eng.* **20**, 1685–1695 (1984)
27 Dvorkin, E. N. and Petöcz, E. G. On the modelling of 2D metal forming processes using the flow formulation and the pseudo-concentrations technique, *Proc. Third Int. Conf. on Computational Plasticity* (Eds D. R. J. Owen *et al.*), Pineridge Press, Swansea, pp. 1037–1052 (1992)